Dynamic Properties of a Model Polymer/Metal Nanocomposite: Gold Particles in Poly(*tert*-butyl acrylate)

Douglas H. Cole,[†,‡] Kenneth R. Shull,*[,‡] Peter Baldo,[†] and Lynn Rehn[†]

Materials Science Division, Argonne National Laboratory, Argonne, Illinois 60439, and Department of Materials Science and Engineering, Northwestern University, Evanston, Illinois 60208

Received August 7, 1998

ABSTRACT: A combination of methods has been used to study the dynamic properties of a nanocomposite consisting of evaporated gold particles embedded in poly(*tert*-butyl acrylate). Rutherford backscattering spectrometry was used to measure the diffusion coefficients of the gold particles and of the polymer molecules; dewetting experiments were used to probe the viscosity of thin films with and without gold particles. The gold particles diffused with a temperature dependence similar to the temperature dependence of the polymer viscosity, but with hydrodynamic radii that greatly exceeded the actual radii of the gold particles. The gold particles also increased the viscosity of a low molecular weight polymer film by a factor of 4. Our interpretation of these results is that long-lived polymer bridges between individual gold particles stabilize clusters with dimensions of approximately 50 nm. A geometrical model of the bridging process was also developed. Results from this model can readily be applied to homogeneous nanoparticle dispersions in polymeric matrixes.

1. Introduction

Dispersions of very small metal particles in polymeric matrixes are scientifically and technologically important for a variety of reasons. One potential advantage of a dispersed particle system is that many of its properties are strongly dependent on the interfacial properties of the material, simply because the fraction of the overall material which is in the vicinity of an interface is quite high. Consider the effect of an interface on the glass transition temperature of a polymer. Recent experimental investigations have indicated that the glass transition temperature of a very thin polymer film can be either higher or lower than the glass transition temperature of the bulk material and that the nature of the substrate plays an important role in this effect.[1−8] Similar effects have been observed in polymer solutions, where the dynamics of polymer adsorption and desorption are much slower than one would expect based only on the concentration of polymer molecules at the interface.[9,10] These experiments have probed individual thin films, using techniques such as X-ray reflectivity, ellipsometry, or infrared spectroscopy. Because of the increased interfacial area, many of these effects will readily apparent in a nanoparticle dispersion.

In addition to simply providing a large interfacial area, dispersions of very small inorganic particles may have useful electronic, optical, or magnetic properties.[11−16] Many of these properties, such as superparamagnetism in magnetic materials[17−20] or tunable band gaps in quantum dot semiconductor arrays,[21,22] require that particle sizes and interparticle spacings be in the nanometer range. Because of the similarity of these dimensions to the typical sizes of polymeric molecules, there is considerable interest in using polymeric materials to control the sizes and distributions of nanoparticle dispersions. One approach that has been employed by several groups is to use ordered block copolymers as templates for controlling the distributions of the metal particles.[23−29] Unfortunately, the morphology of the underlying polymeric template and the morphology of the resultant particle dispersion are not related to each other in a completely straightforward way. For example, while one would prefer to have one metal particle per spherical domain in an ordered diblock copolymer, there are typically several very small particles in each domain. This result can be at least partially explained in terms of kinetic limitations on particle coalescence which can be attributed to the presence of the polymer molecules. Spatz et al. have shown that by circumvention these kinetic limitations in solvent-cast films, it is possible to obtain well-ordered arrays of metal particles with controlled sizes.[29]

For practical reasons it is convenient to process nanocomposite materials when the polymer is in the melt state. In these situations a more fundamental understanding of the dynamic properties is required. Such properties include, for example, the viscosity of the composite medium and the diffusive properties of the individual particles in the polymer matrix. While much of the scientific interest in this area involves the use of block copolymers, the most fundamental questions can be more readily addressed by conducting experiments with homopolymers. The factors which control the coalescence of metal particles in an individual block copolymer domain, for example, are very similar to the factors which control particle coalescence in the corresponding homopolymer.

We have found that gold particles in a poly(*tert*-butyl acrylate) (PTBA) matrix form an excellent model system for studying the fundamental properties of polymer/metal nanocomposite systems.[30,31] PTBA is an amorphous polymer with a glass transition temperature near 50 °C. The polymer is not prone to photooxidation, although severe thermal oxidation to poly(acrylic acid) begins to occur at temperatures above about 160 °C.[32] Nanocomposites are formed by thermal evaporation of a discontinuous gold layer onto a thin film of PTBA. In our experiments, the gold coverage is equivalent to a continuous layer of gold with a thickness of 0.4 nm. The

[†] Argonne National Laboratory.
[‡] Northwestern University.

10.1021/ma981252b CCC: $18.00
Published on Web 01/14/1999

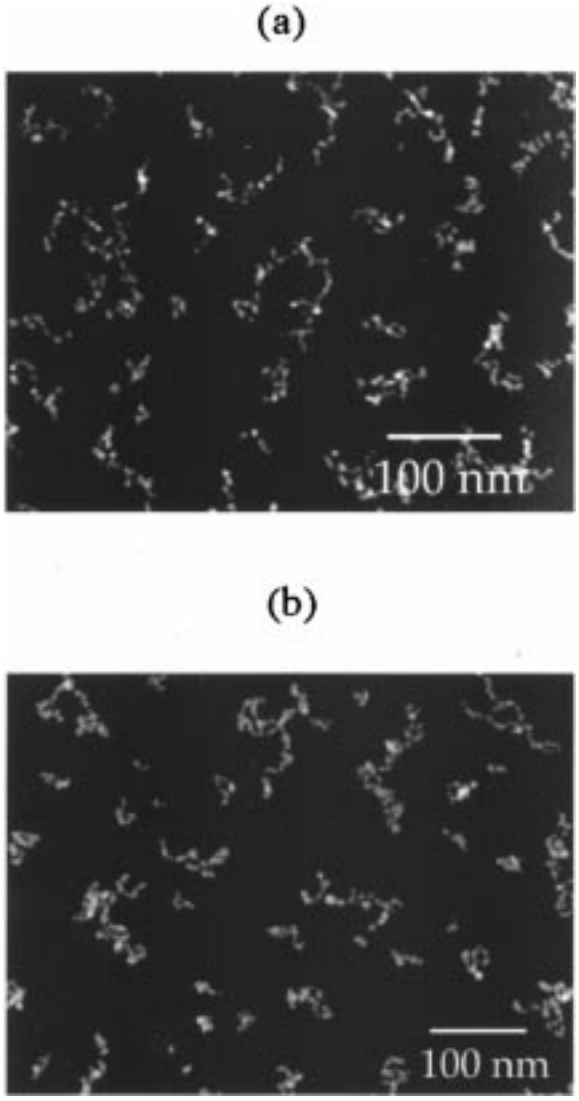

Figure 1. TEM micrographs illustrating the characteristic morphology after various annealing treatments for gold particles in a deposited on PTBA with a molecular weight of 100 000: (a) after annealing for 1 h at 90 °C; (b) after annealing for 8 h at 90 °C.

as-deposited layer consists of individual gold particles with diameters of approximately 1 nm. During annealing treatments, the gold particles quickly coalesce and form aggregates of slightly larger particles, similar to those shown in Figure 1. Because the qualitative features of the particle morphology do not change substantially during subsequent annealing treatments, this figure accurately represents the structure of the polymer/metal nanocomposites which we are investigating as part of this work. There are two distinguishing features of these dispersions which are particularly important to what follows. First, individual gold particles form aggregates with dimensions of approximately 50 nm. The spacing between these aggregates is generally larger than the dimensions of individual polymer molecules. The second feature of these dispersions is that the distances between particles within an aggregate are typically much less than the dimensions of individual polymer molecules.

The close proximity of the particles within the aggregates is the key distinguishing feature of the dispersions. This feature enables us to make the connection to some of the interfacial properties mentioned above. Because the particles are so close to each other, individual polymer molecules will simultaneously be in contact with more than one particle, forming "bridges" between these particles. If the exchange of polymer segments at the polymer/metal interface is slow in comparison to experimental time scales, these bridges can be viewed as permanent links tying individual gold particles to one another. A slowing down of the exchange kinetics at the polymer/metal interface is consistent with an increase in the glass transition temperature in the interfacial regime. The qualitative effect of these slow exchange kinetics is the subject of a letter which has been published previously.[30] Our purpose here is to present a more comprehensive description of the properties of these dispersions, including the mobilities of the particles and the polymer molecules, and the overall viscosity of the composite medium. We begin in the next section with a generalized treatment of bridging in dispersed particle systems, based on purely geometrical considerations. The results and discussion section which follows contains four parts. First we present a thorough characterization of the PTBA polymers used in our experiments. Next, we describe results obtained from marker motion experiments which are designed to probe the diffusive properties of the polymer molecules themselves. Following this, we describe results obtained for the diffusion of the gold particles. We then describe a set of dewetting experiments designed to determine the overall viscosity of the polymer/gold composite system. We conclude with an overall picture of the properties of the dispersions which accounts for all of the results which have been obtained.

2. Geometrical Considerations

Because bridging interactions are found to be important in determining many of the overall properties of the nanoparticle dispersions, it is important to understand under what conditions these bridges will exist. Qualitatively, it is obvious that a transition between bridging to nonbridging will take place for particle separations which are similar to R_g, the radius of gyration of an individual polymer molecule. The radius of gyration is related to the statistical segment length, a, by the following expression:

$$R_g = a\left(\frac{N}{6}\right)^{1/2} \tag{1}$$

Here N is the degree of polymerization, obtained by dividing the polymer molecular weight (M) by the molecular weight of a repeat unit (M_0). For PTBA $M_0 =$ 128 and $a \approx 0.7$ nm.[33] Values of R_g for the polymers used in this study range from 2.1 nm ($M = 7\,000$) to 16 nm ($M = 400\,000$). By inspection of the micrographs shown in Figure 1, it is easy to see that bridging will take place between particles in an individual aggregate for all polymer molecular weights but that bridging from one aggregate to another is unlikely for all but the highest molecular weight polymers.

Our goal in this section is to go beyond this simple qualitative picture and to develop a methodology for quantifying the extent of bridging between isolated particles. One must keep in mind that the arguments presented here are purely geometrical. Imagine that a snapshot of the system is taken at a particular instant in time, and that the conformations of all the individual molecules are somehow recorded. Any molecule in this

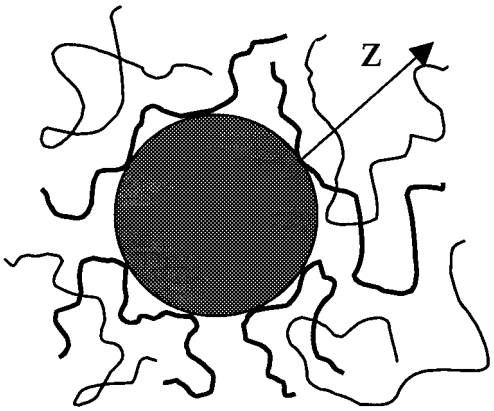

Figure 2. Schematic illustration distinguishing between polymer molecules which are in contact between particles (thick lines) and polymer molecules which are not in contact with a particle (thin lines). The arrow illustrates the definition of z as the distance from the particle surface.

snapshot which is in contact with more than one particle is defined as a "bridge". In subsequent sections we will assume that the lifetimes of these bridges must be relatively long, but at this point we are only interested in the number of these bridges which are present at any given time. This sort of statistical information can be easily obtained by lattice models similar to those used by DiMarzio,[34] Scheutjens and Fleer,[35−37] and many others. While different kinds of information can be obtained from these models, we are particularly interested in the local volume fraction of a polymer melt corresponding to molecules which have at least one segment in contact with a spherical particle at a specified location. The situation is as illustrated in Figure 2. In this example, polymer molecules which are in contact with an isolated spherical particle are distinguished (drawn in bold) from molecules which are not in contact with the particle. We refer to the molecules which have at least one segment in contact with the particle as the "contact chains", whereas the remainder of the molecules are referred to as the "noncontact" chains. The local volume fraction of contact chains is ϕ_c. This volume fraction is obtained as a function of z, the distance from the particle surface, by solving the appropriate set of equations. The numerical approach which we use to calculate the relevant volume fraction profiles is very similar to the procedure which has been previously applied to a flat interface.[38] The polymer molecules are treated as random walks. These walks can begin anywhere in the system, but are only included in the volume fraction profile if they contact a particle at some point. Because we are interested in spherical particles, we use a numerical approach which takes into account the spherical symmetry of the system.[39,40]

When the volume fraction profiles for the contact chains are appropriately normalized by R_g, the results depend only on the ratio between the particle radius, R, and the polymer radius of gyration. Calculated profiles for a variety of R/R_g ratios are plotted in Figure 3. For $R/R_g = \infty$, corresponding to a flat interface, the equilibrium volume profile for the contact chains, $\phi_\infty(z)$, is approximated by the following empirical form:

$$\phi_\infty(z) = \exp\{-0.63(z/R_g)^{-1.76}\} \qquad (2)$$

As the particle radius decreases, the total number of

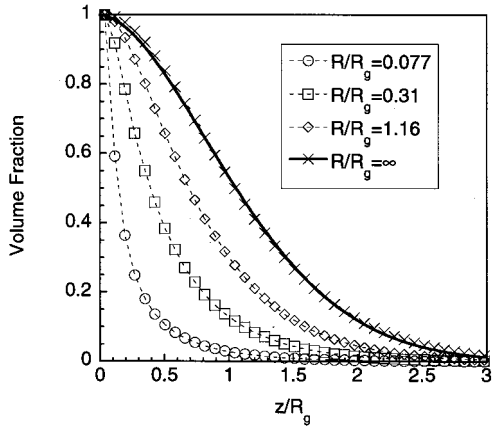

Figure 3. Volume fraction profiles corresponding to polymer molecules with at least one segment in contact with a spherical particle. The different curves correspond-to-different ratios of the particle radius (R) to the radius of gyration (R_g) of the polymer molecules. The line drawn through the points with $R/R_g = \infty$ corresponds to $\phi_\infty(z)$ as given by eq 2.

contact points on the particle surface is reduced, and the volume fraction at a given value of z decreases as well.

One important parameter which can be easily extracted from the volume fraction profiles is the total number of polymer chains which have at least one segment in contact with a particle. This quantity, referred to here as β, is obtained by integration of the volume fraction profile for the contact chains

$$\beta = \frac{1}{V}\int_0^\infty 4\pi z^2\, \phi_c(z)\, dz \qquad (3)$$

where V is the volume occupied by a polymer molecule. It is often more useful to describe β in a more general form, involving the normalized volume fraction profile:

$$\beta = \frac{R_g^3}{V}\int_0^\infty 4\pi (z/R_g)^2\, \phi_c(z/r_g)\, d(z/r_g) \qquad (4)$$

Because the normalized volume fraction profiles for the contact chains depend only on R/R_g, appropriately normalized values of β will also depend only on this quantity. Indeed, values of $\beta V/R_g^3$ calculated for polymers with different degrees of polymerization fall along a single master curve which is shown in Figure 4. Values of β are accurately represented by the following expression:

$$\frac{\beta V}{R_g^3} = 13.3\left(\frac{R}{R_g}\right) + 14.6\left(\frac{R}{R_g}\right)^2 \qquad (5)$$

Note that this expression for β has the correct asymptotic behavior for large values of R, since in this regime curvature effects become unimportant, and β must be proportional to the surface area of the particle, which is in turn proportional to R^2. The number of contact chains per unit area of the particle surface is defined as Σ, with Σ_∞ defined as the value of Σ for a flat interface:

$$\Sigma_\infty = \lim_{R\to\infty}\frac{\beta}{4\pi R^2} = 1.16\frac{R_g}{V} \qquad (6)$$

The same expression can also be obtained by integration of the limiting form of the attached polymer volume

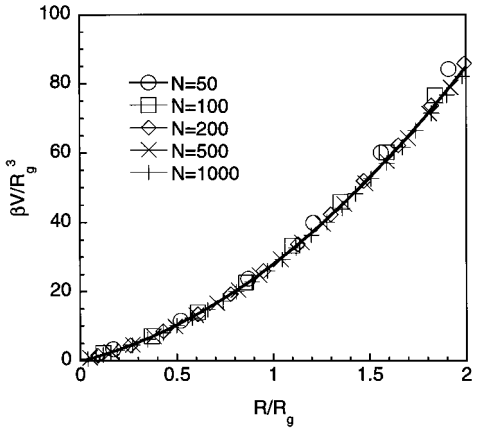

Figure 4. Number of polymer molecules (β) with at least one segment in contact with a spherical particle, as a function of the particle radius (R). We have used normalized units, where R_g is the polymer radius of gyration and V is the volume occupied by an individual polymer molecule. Values for different degrees of polymerization, N, are included to illustrate that there are no significant artifacts arising from the lattice discretization.

fraction for a flat interface (eq 2):

$$\sum_{\infty} = \frac{1}{V}\int_0^{\infty}\phi_{\infty}(z)\,dz = 1.16\frac{R_g}{V} \tag{7}$$

The physical significance of $\sum_{\infty}$ can be viewed in the following way. Suppose that the surface of a completely equilibrated polymer melt is brought into contact with a flat surface which is highly reactive toward the polymer, so that all monomers at the surface of the melt are instantaneously grafted with the surface. The surface concentration of grafted chains in this layer is $\sum_{\infty}$. The equivalent thickness of this layer, defined as the thickness of the polymer layer which would be obtained if all the nongrafted polymer were rinsed away, is $\sum_{\infty}V$, which is equal to $1.16R_g$.

As mentioned above, the results in this section have been presented in an effort to quantify the amount of polymer bridging. Clearly, certain limitations exist which restrict the accuracy of this approach. The numerical treatment assumes that the statistical population of chain conformations is fully equilibrated. This assumption is at odds with our belief that the segmental dynamics at the polymer/metal interface are retarded significantly, so that that bridges between different particles have relatively long lifetimes. This interplay between kinetics and polymer chain conformations introduces other complications as well. For a flat surface, the average number of polymer/substrate contacts scales as $N^{1/2}$. Within the population of contact chains, there will be a statistical distribution of the number of contact points around this mean value. The overall mobility of chains which have only one contact with the surface is expected to be higher than the mobility of chains which have many contacts with the surface. Also, as the particle size decreases (while maintaining a constant degree of polymerization for the polymer chains), the average number of contact points per chain must decrease as well. For low values of R/R_g, the number of contact chains increases linearly with R, but the surface area itself, which determines the total number of available contact points, scales as R^2. Finally, the atomic structure of the polymer molecules themselves places a limit on what can reasonably assumed for the particle radius. Any polymer segment within a persistence length of the surface should be considered as being in contact with the surface. The persistence length of the polymer (approximately 1 nm for most amorphous polymers) sets a lower bound on what can meaningfully be used as the particle radius in these calculations.

Given the limitations described in the previous paragraph, we conclude this section with a useful qualitative description of interparticle bridging. Our basic picture is that polymer bridges are able to tie different particles to one another. An analogy is made to the nonlinear step growth polymerization of reactive monomers. The number of different reactions that can take place between a given monomer and surrounding molecules is its functionality. In our case, the analogues of the monomers are the individual particles. The analogue of the functionality is β, because this quantity determines the number of different molecules which are able to link a given particle with its neighbors by the formation of bridges. In treatments of polymerization reactions, the extent of reaction is defined as the probability that a given functional group has reacted. The appropriate substitute for the extent of reaction in our case is related to the volume fraction of contact chains at a distance corresponding to the interparticle separation. Specifically, we need to replace the extent of reaction by $\alpha\phi_c(d)$, where d is the interparticle spacing and α is the number of particles at this distance which are suitably situated for bridging with a given bridging molecule. The actual value of α will depend on the spatial arrangement of particles. For our purposes α can be viewed as a correction factor which is not substantially different from one.

The analogy between particle bridging interactions and nonlinear step growth polymerization can now be competed by writing down the appropriate analogue of the Carothers equation.[41] In our case, this equation gives $\bar{N}_n$, the average number of particles in a cluster of particles which is bound together by bridging molecules:

$$\bar{N}_n = \frac{2}{2 - \phi_c(d)\alpha\beta} \tag{8}$$

Taking $\bar{N}_n = \infty$ as an approximate criterion for the percolation threshold, we see that the bridged particles will form a continuous network for $\phi_c(d)\alpha\beta = 2$. By substitution of appropriate values for the density of the PTBA (≈ 0.9 g/cm^3) and its statistical segment length (≈ 0.7 nm), eq 5 for β can be cast in the following form:

$$\beta_{ptba} = 4.73R + 205M^{-1/2}R^2 \tag{9}$$

R is the particle radius in nanometers, M is the polymer molecular weight, and the ptba subscript indicates that this equation applies specifically to PTBA. For particles with $R = 2$ nm (typical of the particle radii for our model dispersions), β_{ptba} ranges from 11 for the polymer with $M = 400\,000$ to 19 for the polymer with $M = 7\,000$. Given the relatively small dependence of β on M, we can take $\beta = 15$ as a representative value and assume that the percolation threshold for a collection of small 2 nm gold particles in PTBA occurs if $\phi_c(d)$ exceeds $2/15 = 0.13$. As illustrated by the curves shown in Figure 3, this volume fraction corresponds to a particle separation between R_g and $2R_g$, with the specific

value depending on R/R_g. Clearly, the particle spacing within one of the clusters shown in Figure 1 is small enough so that bridging interactions will exist. Particle bridging between different clusters does not appear likely, with the possible exception of the highest molecular weight polymers. If the segmental exchange kinetics at the polymer/metal interface are sufficiently slow, one would expect the system to behave as if it consisted of independent clusters with sizes of approximately 50−100 nm. In the following sections, we see that this picture is consistent with the observed behavior of the metal particle dispersions which we have studied.

3. Results and Discussion

3.1. Polymer Characterization. A variety of PTBA polymers with molecular weights between 7 000 and 400 000 were synthesized by anionic polymerization as described previously.[42] The glass transition temperatures, T_g, for these polymers were measured by differential scanning calorimetry. The T_g values were equal to 49 ± 1 °C, with the exception of the lowest molecular weight polymer (with $M = 7\,000$) which showed a slight depression in T_g to 42 °C.

The temperature dependence of the zero shear viscosity, η_0, was measured for PTBA samples with molecular weights of 55 000 and 7 000. The results for both polymers are accurately represented by the following form of the Vogel equation:

$$\log \eta_0 \text{ (Pa sec)} = A + \frac{706}{T - T_g + 59} \qquad (10)$$

Here, A is a molecular weight dependent fitting parameter, T is the temperature of the sample, and T_g is the glass transition temperature of the polymer. At 60 °C, the viscosity of the polymer with $M = 7000$ ($T_g = 42$ °C) was 15 000 Pa s, giving $A = -4.99$. For the polymer with $M = 55\,000$, ($T_g = 49$ °C), a viscosity of 3 500 Pa s was obtained at 100 °C, giving $A = -2.87$. Because sufficient quantities of polymer with different molecular weights were not available, we obtained an approximation for the molecular weight dependence of A by assuming that at a constant value of $T - T_g$, the zero shear viscosity obeys the following expression:[43]

$$\eta_0 = C_1 M + C_2 M^{3.4} \qquad (11)$$

C_1 and C_2 are obtained by fitting to the viscosity values for the polymers with $M = 7000$ and $M = 55\,000$. Reasonable values can be obtained for these constants because the low molecular weight polymer is in the linear regime, and gives C_1, and the higher molecular weight polymer is in the entangled regime (or very close to it) and gives C_2. In this way, we obtain the following expression for the molecular weight dependence of A:

$$A = \log(1.35 \times 10^{-9} M + 10^{-19} M^{3.4}) \qquad (12)$$

In addition to rheological quantities such as the zero shear viscosity, we are also interested in diffusive properties, both of individual polymer molecules, and of dispersed metal particles. The central quantity relating diffusive and rheological behavior of polymer melts is the monomeric friction coefficient, ζ_0. This quantity can be related to the viscosity of an unentangled polymer melt through the Rouse theory of polymer dynamics.[43] Here ζ_o is related to η_0 by the following expression:

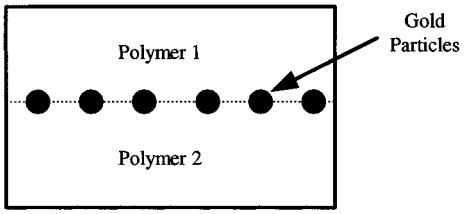

Figure 5. Schematic representations of the samples used for the diffusion experiments.

$$\eta_0 = \frac{\zeta_0 M N_{av} \rho a^2}{36 M_0^2} \qquad (13)$$

Here N_{av} is Avogadro's number and ρ is the polymer density (≈ 0.9 g/cm^3 for PTBA). The following expression for the monomeric friction coefficient is obtained from the viscosity data for the polymer with $M = 7000$:

$$\log \zeta_0 \text{ (kg/s)} = -14.5 + \frac{706}{T - T_g + 59} \qquad (14)$$

3.2. Marker Motion Experiments. To determine if the gold particles affected the diffusion of the polymer molecules, we conducted a set of marker motion experiments. These experiments were similar to those conducted by Green et al. with the polystyrene/gold system,[44] and began with the creation of bilayer samples as depicted in Figure 5. The samples consisted of gold particles placed between PTBA layers with different molecular weights. The first layer was spun-cast on a polished silicon wafer, and a discontinuous, 0.4 nm marker layer of gold was thermally evaporated on top of it. The second polymer layer was floated onto a water bath and placed on the first layer of polymer. For one sample the higher molecular weight polymer (M = 400 000) was placed against the substrate and a lower molecular weight polymer ($M = 7000$ or $M = 21\,000$) was at the free surface. The second sample reversed this geometry, with the lower molecular weight film directly against the substrate. In both cases, the interface moved toward the low molecular weight layer, as would be expected from its larger diffusion coefficient.

Analysis of the marker motion experiments was straightforward and followed that of Green *et al.*[44] The distance, Δx, traversed by the marker layer is given by

$$\Delta x = C\sqrt{D^* t} \qquad (15)$$

where C is a constant related to the ratio of diffusion coefficients of the two polymer layers, D^* is the tracer-diffusion coefficient of the lower molecular weight polymer, and t is the annealing time. In our case, the diffusion constants of the two polymers are very different, and C can be assumed to be equal to the limiting value of 0.48 for a divergent ratio of diffusion coefficients. Evaluating the marker motion as a function of time reveals that the marker displacement scales as $t^{1/2}$ and that there is no preference for the markers to move toward the substrate or toward the free surface. Data for the case where the lower molecular weight polymer has $M = 21\,000$ are shown in Figure 6. The corresponding diffusion coefficient obtained from eq 15 is 1.8 × 10^{-14} cm^2/s.

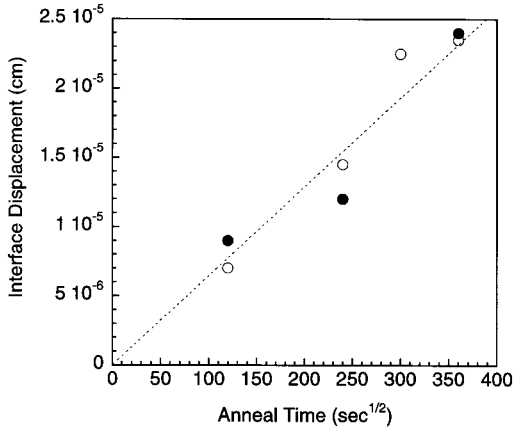

Figure 6. Time dependence of the displacement of the gold in a marker motion experiment. The molecular weights of the two PTBA layers are 21 000 and 400 000, and the diffusion temperature is 60 °C. Open circles represent the case where the high molecular weight polymer is adjacent to the substrate. Filled circles represent the opposite case, where the high molecular weight polymer is adjacent to the free surface. The dashed line is a fit to eq 15, with $C = 0.48$ and $D = 1.5 \times 10^{-14}$ cm^2/s.

The monomeric friction coefficient, ζ_0, is obtained from the following expression for the self-diffusion coefficient, which is valid for polymers in the unentangled regime:[45]

$$D = \frac{k_B T M_0}{M \zeta_0} \tag{16}$$

From this expression we obtain a monomeric friction coefficient of 1.6×10^{-5} kg/s for PTBA at 60 °C. This value should be compared to a value of 3.8×10^{-5} kg/s which is obtained from the measured viscosity at 60°, according to eq 13. The two values of ζ_0 differ by a factor of about two, which is typical of the agreement observed by previous investigators.[44−46] The difference between the two values of the friction coefficient is greater for experiments where the low molecular weight polymer has $M = 7000$. As discussed previously, this discrepancy can be attributed largely to the depression in the glass transition temperature for the polymer with $M = 7000$.[30] Our primary conclusion from the marker motion experiments is that the gold particles do not present a substantial impediment to the motion of polymer molecules. This result is not surprising, given the nature of the gold particle layers. As illustrated in Figure 1, substantial gaps exist between gold clusters through which polymer molecules can easily diffuse. Nevertheless, this result is an important one to keep in mind as we discuss our results on the diffusion of the particles themselves. As discussed in the following section, dramatic effects on the mobility of the gold particles are observed.

3.3. Particle Diffusion. Having established that the gold particles present no significant interference to the diffusion of polymer molecules, we now examine the ability of the particles themselves to diffuse. Samples used in these experiments were similar to those used for the marker motion measurements, but with identical polymers used for the layers on either side of the gold particles. Diffusion coefficients for the gold particles were obtained by comparing the gold depth distributions measured by RBS to the appropriate solutions to the diffusion equation, accounting for the depth resolution

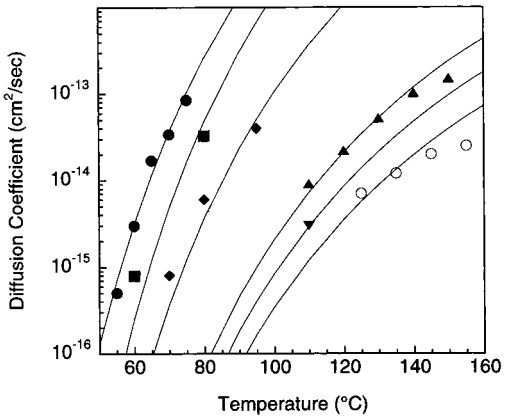

Figure 7. Temperature dependence of of the gold particle diffusion coefficients for the following molecular weights: $M = 7000$ (●), $M = 21\,000$ (■), $M = 50\,000$ (◆), $M = 77\,000$ (▲), $M = 81\,000$ (▼) and $M = 100\,000$ (○). The dashed lines are fits to the Stokes−Einstein equation (eq 17), using viscosities calculated from eqs 10 and 12 and the effective particle radii listed in Table 1.

Table 1. Effective Hydrodynamic Radii Obtained from the Diffusion Coefficients of the Gold Particles

M	T_g (°C)	R (nm)
7 000	42	50
21 000	49	10
50 000	49	10
77 000	49	120
81 000	49	250
100 000	49	300

of the technique.[30,31] Gold particle diffusion coefficients were obtained as a function of temperature for polymers with molecular weights ranging from 7000 to 100 000. The results of these experiments are shown in Figure 7, where the temperature dependence is plotted for each of six different molecular weights used in these experiments.

A convenient way to analyze the data is by comparison to the Stokes−Einstein equation for diffusion of isolated spherical particles in a viscous medium:

$$D = \frac{k_B T}{6\pi\eta_0 R} \tag{17}$$

where R is the radius of the particle. In our case, R is an "effective" radius determined for each polymer molecular weight. These empirical fits are represented by the solid lines in Figure 7, and correspond to the effective radii which are listed in Table 1. Values for η_0 in eq 17 were obtained from eqs 10 and 12. The analysis here in terms of the Stokes−Einstein equation is instructive. Note that the values of the effective hydrodynamic radius determined in this way are quite large, varying from 10 to 300 nm.[47] The highest of these values is 2 orders of magnitude larger than the actual mean particle radius. These values are roughly consistent with the sizes of the particle aggregates shown in Figure 1, however. Our interpretation of these results is that the particles diffuse as aggregates which are held together by bridging interactions. Other experiments using colloidal gold suggest that reducing the concentration of particles to the point where the interparticle spacing far exceeds typical polymer chain dimensions leads to fewer bridging interactions and better agreement with the Stokes−Einstein predictions based on actual particle dimensions.[48]

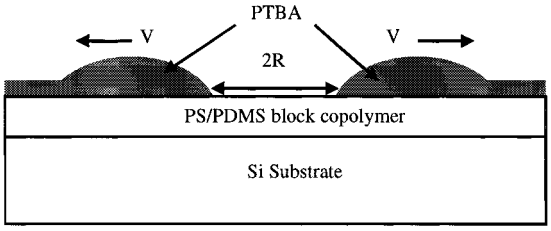

Figure 8. Schematic illustration of the dewetting process, showing the growth of a circular dry patch of radius R.

3.4. Viscosity Measurements of a Thin-Film Nanocomposite. The experiments described in the previous sections provide information about the mobilities of the polymer molecules, and of the gold particles. To obtain information pertaining to the properties of the overall composite system, we have conducted a series of dewetting experiments. A schematic illustration of the dewetting process is shown in Figure 8. A thin polymer film is placed on a low energy surface on which the film is thermodynamically unstable. During thermal annealing, circular dry patches form spontaneously throughout the initially homogeneous film. Polymer from an individual dry patch is forced into the surrounding rim, which moves outward with a velocity V. The dewetting of a liquid film of polymer from a substrate has been observed to proceed with a velocity that is inversely proportional to the bulk viscosity of the dewetting fluid.[49] If the assumption is made that the dewetting velocity is determined by a balance between viscous dissipation and surface energetics, the following expression is obtained:

$$V = \frac{k\theta_e{}^3\gamma}{\eta_0} \tag{18}$$

θ_e is the equilibrium contact angle, γ is the surface free energy of the dewetting fluid, and k is a constant which is approximately equal to 3×10^{-8} (with θ_e expressed in deg).

Poly(dimethyl siloxane) (PDMS) is an ideal low surface-energy substrate for conducting the dewetting experiments. It is important to use a very thin film of PDMS, so that viscoelastic losses in the dewetting film do not limit the dewetting velocity.[50,51] In our case a 100 nm layer of a symmetric polystryene/PDMS block copolymer, cast on a polished silicon wafer, was used as the substrate. Because of the much lower surface free energy of PDMS in comparison to polystyrene, an essentially pure PDMS layer is expected to exist at the surface of the block copolymer film.[52,53] Dewetting experiments were carried out by placing the samples in a heating stage and viewing the dewetting process with an optical microscope attached to a video recorder. The temperature was kept below 95 °C in order to maintain the polystyrene domains of the block copolymer in the glassy state. The dewetting film was a 100 nm layer of PTBA with a molecular weight of 7000. This film was spun cast onto a glass slide, carefully floated onto a water bath, and picked up on the block copolymer substrate. The dewetting behavior of PTBA control films, with no gold evaporated on the top surface, was compared to the dewetting behavior of films with gold particle layers identical to those used in the particle diffusion and marker motion experiments.

The radius of a circular dry patch in a control film as a function of time at 80 °C is plotted in Figure 9. The

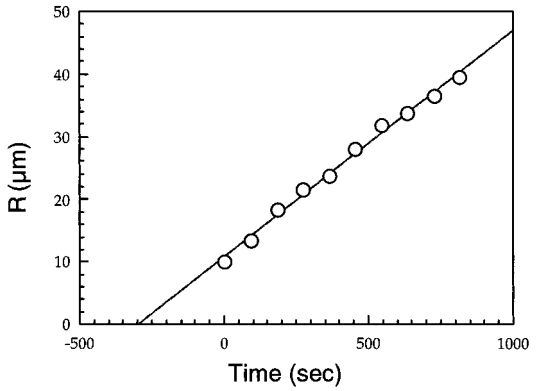

Figure 9. Dry patch radius vs time at 80 °C for a PTBA polymer ($M = 7000$) on a polished silicon substrate which has been coated with a PS/PDMS diblock copolymer.

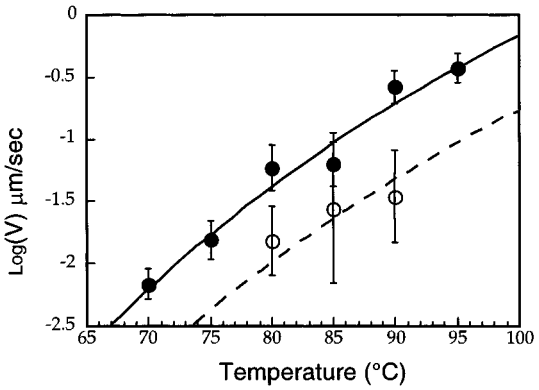

Figure 10. Dewetting velocity vs temperature for PTBA ($M = 7000$) on the PDMS -treated substrates. Filled circles represent samples without gold deposition, and open circles have 0.4 nm of gold evaporated on to the sample surface. The lines represent the prediction of eq 18, assuming $\gamma = 27$ mJ/m^2 and $k\theta_e{}^3 = 3 \times 10^{-4}$. For the solid line, the actual values of the polymer viscosity are used. A larger viscosity (by a factor of 4) is used to give the dashed line.

dewetting velocity for this particular sample, obtained from the slope of this plot, is 0.036 μm/s. We are interested in comparing the temperature dependence of this dewetting velocity for PTBA control films and for PTBA films which have a layer of gold particles evaporated onto the top surface. This comparison is shown in Figure 10. The lines in this figure are fits to eq 18, assuming $\gamma = 27$ mJ/m^2 and $k\theta_e{}^3 = 3 \times 10^{-4}$. The quantity $k\theta_e{}^3$ is used as a fitting paramter in our experiments, since we are interested only in the relationship between the viscosity of the thin films and the dewetting velocity. The solid line uses the actual values for the PTBA viscosity, and the dashed line uses viscosities which are four times larger than the actual values.

Our conclusion from the dewetting experiments using the polymer with $M = 7000$ is that the gold particles increase the effective viscosity of this polymer by a factor of 4. The assumptions made here are that the dewetting experiments are indeed measuring the viscosity, and that $k\theta_e{}^3$ is not affected by the presence of the gold particles. The first assumption certainly seems reasonable, since the dewetting velocity for the control sample (without gold particles) is indeed inversely proportional to the viscosity of the polymer. The second assumption also seems reasonable, since we have determined independently from depth profiling measurements using Rutherford backscattering spectrometry that the gold

particles do not segregate to either the free surface or the substrate. Therefore, the particles are not expected to affect the energy balance which determines the equilibrium contact angle.

4.4. Overall Picture. Our overall picture of the nanoparticle dispersions discussed here is that metal particles within an individual aggregate are bound together over relatively long time scales by polymer molecules which bridge the gap between individual particles. The aggregates form very early in the annealing process and have dimensions of approximately 50 nm. This picture is consistent with the results described in each of the previous three subsections. Because the aggregates are quite widely spaced, molecules can easily pass from one side of the gold layer to the other. As a result, the gold particles can be treated as inert markers which allow accurate values to be obtained for the diffusion coefficients of polymer molecules. Because the lifetimes of the bridges are relatively large, the diffusion coefficients of the gold particles themselves correspond to the diffusion of entire aggregates. Indeed, the effective hydrodynamic radii obtained from the diffusion measurements are consistent with the observed aggregate size. The relatively long lifetimes of the aggregates also explain why nearly Fickian diffusion is observed in all cases, i.e., diffusion coefficients which are independent of the annealing time. As diffusion progresses, the particle distribution broadens, and the average particle concentration decreases. The decrease in average particle concentration corresponds to an increased separation between aggregates, however, and not to a change in the aggregate size. For this reason the diffusion coefficient remains essentially independent of concentration, and Fickian diffusion is observed.

The measured changes in the thin-film viscosity also agree with our picture of long-lived aggregates. Here we make an analogy to the viscosity of suspensions, where the inclusion of hard spheres at a volume fraction of 30% increases the viscosity of a liquid by a factor of 4.[54] Clearly, the flexible, two-dimensional aggregates of metal particles responsible for the increased viscosity in our case are different, and may show larger effects at lower volume fractions. Conceptually, however, the effect on the viscosity is similar, and we believe the analogy to suspensions is a useful one. Certainly, the effect on the viscosity is much larger than what would be predicted from the actual volume fraction of gold, which is less than 1%.

Finally, while our picture of long-lived bridging interactions explains most of the behavior we have observed experimentally, the bridging lifetimes are clearly not infinite. For example, some rearrangement of existing bridges must occur in the very early stages of the annealing process, as the aggregates are being formed. If the dynamics of segmental exchange are slow enough so that the bridges are truly permanent from the very beginning, the particle morphology would not change, (aggregates would not be formed), and no particle diffusion would be observed. Also, we have conducted preliminary experiments which show that the gold particles segregate preferentially to the interface between PTBA and poly(2-vinylpyridine). Some segmental exchange must be possible in order for the gold particles to be exposed to the PVP in the first place. In fact, the PTBA system is one of the few systems we have examined where measurable diffusion is actually observed. We believe that this is because the interactions between PTBA and gold are actually relatively weak, so that some segmental exchange at the polymer/metal interface is possible. Nevertheless, the dynamics are slow enough so that the lifetimes of the bridges dominate much of the behavior of this system.

5. Conclusions

The key message of this paper is a relatively simple one; segmental dynamics at the PTBA/gold interface are slow. As a result, bridges formed by molecules in contact with more than one particle have relatively long lifetimes. Hence the metal particles diffuse as aggregates which are held together by bridging molecules. These aggregates increase the viscosity of the system by an amount which is far beyond what would be expected from the volume fraction of gold particles alone. For homogeneous dispersions of spherical particles, we have developed a formalism which allows the number of bridges to be calculated. Key parameters in the theory include the number of polymer molecules with at least one segment in contact with the interface, and the probability that these molecules reach a second particle at a specified location. From these quantities, one can estimate the location of the percolation threshold, where a continuous aggregate spans the entire sample.

Acknowledgment. This work was supported by the U.S. Department of Energy, BES-Materials Sciences, under Contract No. W31-109-ENG-38.

References and Notes

(1) Wallace, W. E.; Tan, N. C. B.; Wu, W. L.; Satija, S. *J. Chem. Phys.* **1998**, *108*, 3798.
(2) van Zanten, J. H.; Wallace, W. E.; Wu, W. L. *Phys. Rev. E* **1996**, *53*, R2053.
(3) Keddie, J. L.; Jones, R. A. L. *Isr. J. Chem.* **1995**, *35*, 21.
(4) Wallace, W. E.; van Zanten, J. H.; Wu, W. L. *Phys. Rev. E* **1995**, *52*, R3329.
(5) Wallace, W. E.; Wu, W. L. *Appl. Physics Lett.* **1995**, *67*, 1203.
(6) Wu, W. L.; van Zanten, J. H.; Orts, W. J. *Macromolecules* **1995**, *28*, 771.
(7) Keddie, J. L.; Jones, R. A. L.; Cory, R. A. *Europhys. Lett.* **1994**, *27*, 59.
(8) Keddie, J. L.; Jones, R. A. L.; Cory, R. A. *Faraday Discuss.* **1994**, 219.
(9) Schneider, H. M.; Granick, S. *Macromolecules* **1992**, *25*, 5054.
(10) Frantz, P.; Granick, S. *Macromolecules* **1994**, *27*, 2553.
(11) Siegel, R. W. *Mater. Sci. Eng. A* **1993**, *168*, 189.
(12) Vassiliou, J. K.; Mehrotra, V.; Russell, M. W.; Giannelis, E. P. *J. Appl. Phys.* **1993**, *73*, 5109.
(13) Nimtz, G.; Enders, A.; Marquardt, P.; Pelster, R.; Wessling, B. *Synth. Met.* **1991**, *45*, 197.
(14) Perenboom, J. A. A. J.; Wyder, P. *Phys. Rep.* **1981**, *78*, 173.
(15) Kreibig, U.; Cenzel, L. *Surf. Sci.* **1985**, *156*, 678.
(16) Nguyen, H. U.; Collins, R. W. *J. Opt. Soc. Am. A* **1993**, *10*, 515.
(17) McMichael, R. D.; Shull, R. D.; Swartzendruber, L. J.; Bennett, L. H. *J. Magn. Magn. Mater.* **1992**,
(18) Roy, S.; Das, D.; Chakravorty, D.; Agrawal, D. C. *J. Appl. Phys.* **1993**, *74*, 4746.
(19) Chen, D. Y.; Patel, S.; Shaw, D. T. *J. Magn. Magn. Mater.* **1994**, *134*, 75.
(20) Morup, S.; Tronc, E. *Phys. Rev. Lett.* **1994**, *72*, 3278.
(21) Edwards, H. L.; Niu, Q.; Delozanne, A. L. *Appl. Phys. Lett.* **1993**, *63*, 1815.
(22) Salata, O. V.; Dobson, P. J.; Hull, P. J.; Hutchison, J. L. *Appl. Phys. Lett.* **1994**, *65*, 189.
(23) Sankaran, V.; Cummins, C. C.; Schrock, R. R.; Cohen, R. E.; Silbey, R. J. *J. Am. Chem. Soc.* **1990**, *112*, 6858.
(24) Chan, Y. N. C.; Schrock, R. R.; Cohen, R. E. *Chem. Mater.* **1992**, *4*, 24.
(25) Cummins, C. C.; Schrock, R. R.; Cohen, R. E. *Chem. Mater.* **1992**, *4*, 27.
(26) Chan, Y. N. C.; Schrock, R. R.; Cohen, R. E. *J. Am. Chem. Soc.* **1992**, *114*, 7295.
(27) Chan, Y. N. C.; Craig, G. S. W.; Schrock, R. R.; Cohen, R. E. *Chem. Mater.* **1992**, *1992*, 885.

(28) Morkved, T. L.; Wiltzius, P.; Jaeger, H. M.; Grier, D. G.; Witten, T. A. *Appl. Phys. Lett.* **1994**, *64*, 422.
(29) Spatz, J. P.; Roescher, A.; Moeller, M. *Adv. Mater.* **1996**, *8*, 337.
(30) Cole, D. H.; Shull, K. R.; Rehn, L. E.; Baldo, P. *Phys. Rev. Lett.* **1997**, *78*, 5006.
(31) Cole, D. H.; Shull, K. R.; Rehn, L. E.; Baldo, B. *Nucl. Instrum. and Methods B*. **1998**, *138*, 283.
(32) Litmanovich, A. D.; Cherkezyan, V. O. *Eur. Polym. J*. **1984**, *20*, 1041.
(33) *Polymer Handbook, 3rd ed.;* Brandrup, J., Immergut, E. H., Eds. Wiley: New York, 1989.
(34) DiMarzio, E. A.; McCrackin, F. L. *J. Chem. Phys.* **1965**, *43*, 539.
(35) Scheutjens, J. M. H. M.; Fleer, G. J. *J. Phys. Chem.* **1979**, *83*, 1619.
(36) Scheutjens, J. M. H. M.; Fleer, G. J. *J. Phys. Chem.* **1980**, *84*, 178.
(37) Fleer, G. J.; Stuart, M. A. C.; Scheutjens, J. M. H. M.; Cosgrove, T.; Vincent, B. *Polymers at Interfaces*; Chapman and Hall: London, 1993.
(38) Shull, K. R. *Macromolecules* **1996**, *29*, 8487.
(39) Leermakers, F. A. M.; Scheutjens, J. M. H. M. *J. Phys. Chem.* **1989**, *93*, 7417.
(40) Shull, K. R. *Macromolecules* **1993**, *26*, 2346.
(41) Young, R. J.; Lovell, P. A. *Introduction to Polymers*; Chapman and Hall: London, 1991.
(42) Ahn, D.; Shull, K. R. *Macromolecules* **1996**, *29*, 4381.
(43) Ferry, J. D. *Viscoelastic Properties of Polymers*; J. Wiley and Sons: New York, 1980.
(44) Green, P. F.; Palmstrøm, C. J.; Mayer, J. W.; Kramer, E. J. *Macromolecules* **1985**, *18*, 501.
(45) Graessley, W. W. *Adv. Polym. Sci.* **1982**, *47*, 67.
(46) Pearson, D. S.; Fetters, L. J.; Graessley, W. W.; Strate, G. V.; Vonmeerwall, E. *Macromolecules* **1994**, *27*, 711.
(47) The effective radii differ slightly from the values given in refs 30 and 31 because the assumptions made here about the molecular weight dependence of the viscosity are slightly different than the assumptions made in these previous references.
(48) Shull, K. R.; Kellock, A. J. *J. Polym. Sci., Polym. Phys.* **1995**, *33*, 1417.
(49) Redon, C.; Brochard-Wyart, F.; Rondelez, F. *Phys. Rev. Lett.* **1991**, *66*, 715.
(50) Shanahan, M. E. R.; Carré, A. *Langmuir* **1995**, *11*, 1396.
(51) Long, D.; Ajdari, A.; Leibler, L. *Langmiur* **1996**, *12*, 1675.
(52) Green, P. F.; Christensen, T. M.; Russell, T. P.; Jérôme, R. *J. Chem. Phys.* **1990**, *92*, 1478.
(53) Chen, X.; Gardella, J. A. *Macromolecules* **1994**, *27*, 3363.
(54) Russel, W. B.; Saville, D. A.; Schowalter, W. R. *Colloidal Dispersions*; Cambridge University Press: Cambridge, England, 1989.

MA981252B